ISSN 1990-7931, Russian Journal of Physical Chemistry B, 2014, Vol. 8, No. 5, pp. 626–633. © Pleiades Publishing, Ltd., 2014.
Original Russian Text © S.A. Tikhonov, I.B. L'vov, V.I. Vovna, 2014, published in Khimicheskaya Fizika, 2014, Vol. 33, No. 9, pp. 11–18.

STRUCTURE OF CHEMICAL COMPOUNDS. SPECTROSCOPY

Photoelectron Spectra and Electronic Structure of Boron Acetylacetonates with Organic Substituents

S. A. Tikhonov, I. B. L'vov, and V. I. Vovna

Far-Eastern Federal University, Vladivostok, Russia

e-mail: lvov.ib@dvfu.ru

Received June 19, 2013

Abstract—Based on experimental data and theoretical results obtained by photoelectron spectroscopy and density functional theory, the electronic structure of the valence levels of boron diethyl acetylacetonate $(C_2H_5)_2BAA$, boron diphenyl acetylacetonate $(C_6H_5)_2BAA$, and 1,2-phenylene dioxyboron acetylacetonate $C_6H_4O_2BAA$ is examined. For the compounds studied, in contrast to F_2BAA, a significant mixing of the π_3 MO of the chelate ring with the orbitals localized on the boron atom, as well as on the $(C_2H_5)_2$, and $(C_6H_5)_2$ fragments, is revealed. The $C_6H_4O_2BAA$ complex is demonstrated to have MOs mainly localized on the oxygen atoms of the $C_6H_4O_2$ fragment. It is shown that the calculated results closely reproduce the experimental sequences of energy levels and the energy intervals between the ionized states of the complex.

Keywords: electronic structure, β-diketonates boron, photoelectron spectroscopy, density functional theory

DOI: 10.1134/S1990793114050108

Chelate compounds belonging to the numerous class of boron β-diketonates are of interest as promising wide-range luminophores $X_2B(O–C(R_1)–C(R_2)–C(R_3)–O)$ [1–4] applicable to biomedicine [5, 6] and chemical technology [7]. An obvious relation between the physicochemical properties of complex compounds and their electronic structure motivates studies of the electronic structure of series of boron complex compounds with specific consumer properties. Establishing structure–property relationships upon substitution with X, R_1, R_2, and R_3 groups enables to synthesize boron complexes with desired properties, such as luminophores for the near-IR range [2]. The most reliable information on the structure of the valence levels can be obtained by means of ultraviolet photoelectron spectroscopy (UVPES) of vaporous compounds in combination with quantum-chemical modeling [8–10].

Previously, we reported the results of a study of the electronic structure of boron difluoride β-diketonates containing substituents with one or two aromatic rings [11–13]. These works demonstrated the changes in the structure of occupied and unoccupied π levels of conjugated cycles that affect the luminescence properties of the complexes. Information obtained from UVPES was used in experimental and theoretical studies of electronic absorption spectra of luminescent complexes [14].

No less relevant and interesting are studies of boron β-diketonates with alkyl and aryl substituents X. These compounds have a high biological activity, and, therefore, they can be used as antiviral agents [5]. In this paper, we report the results of a study of the electronic structure of three boron acetylacetonates X_2BAA (X = C_2H_5 (I), C_6H_5 (II), and *o*-$C_6H_4O_2$ (III) (bidentate group)),

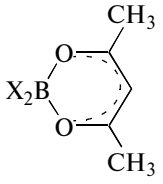

I, II

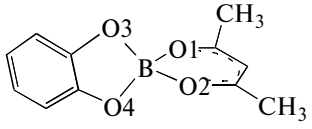

III

by means of the UVPES method and density functional theory (DFT).

This series of compounds is convenient for evaluating the effectiveness of the mixing of the *n* and π orbitals of the β-diketonate cycle with the σ and π orbitals of substituents X, which differ in the geometric position relative to the chelate ring and in the hybridization of carbon atoms in the boron–carbon bond. An interesting feature of 1,2-phenylene dioxyboron acetylacetonate (compound III) is the interaction of the boron atom with four oxygen atoms, interacting, in turn, with various hydrocarbon groups.

Photoelectron spectra of vapors of compounds I–III and the results of quantum-chemical calculations of these compounds in a semiempirical approximation were reported in [15, 16]. Analysis of the calculation results failed to bring them into a satisfactory agreement with the experimental data, which makes the

problem of interpretation of overlapping spectral bands of closely spaced electronic levels still relevant.

EXPERIMENTAL AND CALCULATIONS

The DFT calculations were carried out using the Firefly 7.1.G quantum-chemical code [17], based on the B3LYP5 hybrid exchange-correlation functional and Ahlrichs def-TZVPP basis set (triple-zeta valence plus polarization set with an additional polarization function) [18, 19]. As we demonstrated in [14, 20], this basis is optimal for calculating the characteristics of complexes of metals with β-diketonates. The use of the B3LYP5 functional was motivated by the results of test calculations boron acetylacetonate complexes [14, 20]. To verify whether the optimized structures correspond to local minima on the potential energy surface, the Hessian matrix was calculated.

Ultraviolet photoelectron spectra were recorded on a ES-3201 spectrometer with a He I radiation source ($h\nu = 21.2$ eV) [11, 15, 16]. To maintain an optimal vapor pressure of the test substance, the temperature of the ionization cell was varied from 160 to 220°C. The measured vertical ionization energies (IE) and the energies of the Kohn–Sham orbitals ε were compared using an extended version of the Koopmans theorem: $IE_i = -\varepsilon_i + \delta_i$. The works of Chizhov et al. [21, 22] and our publications on the UVPES of boron difluoride complexes [12, 13] demonstrated that taking into account the dependence of the Koopmans defect δ on the location and composition of the molecular orbital (MO) results in good agreement between the theoretical energies ε_i and experimental IE_i values.

RESULTS AND DISCUSSION

Table 1 lists some calculated geometrical parameters of complexes I–III. Optimization of the geometric parameters of compound I in an asymmetric initial geometry homepage (symmetry group C_1) led to an energy minimum when the ethyl groups were located on both sides of the plane perpendicular to the chelate ring (symmetry group C_2). The total energy of the structure of symmetry C_{2v} in which the chain of atoms $B(C–C)_2$ is located in a plane perpendicular to the chelate ring is 0.38 eV higher than that of the C_2-symmetry structure.

According to calculations, the dihedral angle between the phenyl rings in diphenyl boron complex (II) is 116°; however, the geometry with planar structure of the chelate ring (symmetry C_{2v}) corresponds to a saddle point. Optimization of the geometric parameters without any symmetry restrictions led to a structure with a bend of the chelate ring plane along the O–O line (symmetry C_s). Calculations showed that the energy of the structure with a 19° dihedral angle between the planes of the OCCCO diketonate fragment and OBO fragment is only 66 cm^{-1} below the energy of the saddle point at C_{2v} symmetry. For this reason, when classifying the MO of compound II in Table 2, we used the notations of the irreducible representations of group C_{2v}.

Table 1. Geometric parameters of compounds I–III (bond lengths in Å; angles, in deg)

Bond	R_{AB}			Angle	Angle value, deg		
	I	II	III		I	II	III
B–C/B–O(X)	1.61	1.61	1.44	CBC/OBO	119	116	108
B–O1	1.57	1.55	1.52	O1BO2	106	107	108
O1–C1	1.28	1.28	1.29	O1BX	108	108	110
C1–C3	1.40	1.39	1.39	BO1C1	125	122	125

The geometric structure of 1,2-phenylene dioxyboron acetylacetonate (compound III) strictly corresponds to the symmetry group C_{2v} (the planes of the chelate ring and $C_6H_4O_2$ are orthogonal to each other). The structural parameters of the first coordination sphere of compound III differ from similar characteristics of compounds I and II (Table 1). In particular, the B–O bond length, 1.44 Å, is significantly smaller than the lengths of the B–O1 and B–O2 bonds (1.52 Å).

The ultraviolet photoelectron spectra of the studied compounds feature bands with weak inflections (Fig. 1), which correspond to four-to-seven electronic levels. Expansion of such bands into components in order to determine the energy and type of levels is impossible without a theoretical simulation of ionized states. When expanding the bands in the photoelectron spectra into Gaussian components, we took into account the number of Kohn–Sham orbitals, magnitudes of the energy intervals between them, and close relative ionization cross sections of the electronic levels [12, 13]. When the MO energies were superimposed onto the experimental spectrum, the scale of the calculated values of ε shifted with respect to IE by the mean value of δ. For compounds I and II, III, these value are 2.19 and 2.32 eV, respectively.

Table 2 lists the energy, localization, and type of the molecular orbitals, along with the experimental ionization energies obtained by the expression of the bands into Gaussian components, as well as discrepancies in the values of –ε and IE. In the classification of MOs according to the types of symmetry of the three complexes, we used the irreducible representations of the group C_{2v}. Although the arrangement of the two C_2H_5 groups in compound I lowers symmetry to C_2, in analyzing the MOs localized predominantly on the C_2BAA moiety of I, we also uses the orbital symmetry designations for the point group C_{2v}.

Figures 2 and 3 for compounds I–III show the shape of a number of molecular orbitals of interest for the interpretation of the photoelectron spectra. For compound I, the calculation results, in good agree-

Table 2. Localization of the electron density, MO energies ($-\varepsilon_i$) and experimental IEs for compounds I–III

MO (No, character)	Localization, %			$-\varepsilon_i$, eV	IE_g	δ_i
	B	AA/2O	2X			
Compound I						
34, b_1 ($\pi_3^\beta-\sigma_{CBC}$)	15	47/21	38	6.22	8.50	2.28
33, b_1 ($\pi_3^\beta+\sigma_{CBC}$)	10	52/10	38	7.66	9.79	2.13
32, a_1 (XBX)	19	10/6	71	7.91	10.14	2.23
31, b_2 (n_-^β)	4	83/54	13	8.26	10.42	2.16
30, (2X)	7	3/2	90	8.60	10.75	2.15
29, (2X)	2	14/6	84	8.65	10.82	2.17
28, (2X)	1	4/2	95	9.01	(11.2)	
27, (2X)	3	12/4	85	9.11	(11.3)	
26, a_1 (n_+^β)	7	89/55	4	10.07	(12.3)	
25, a_2 (π_2^β)	1	78/45	21	10.19	(12.4)	
Compound II						
12, b_1 (b_1^-)	1	0	99	5.99	8.36	2.37
8, a_2 (a_2^-)	0	0	100	6.33	8.59	2.26
13, b_2 (a_2^+)	0	0	100	6.47	8.73	2.26
17, a_1 (b_1^+)	2	2/2	96	6.49	8.83	2.34
11, b_1 ($\pi_3^\beta-a_1^-$)	9	61/26	30	6.81	9.07	2.26
10, b_1 ($a_1^-+\pi_3^\beta$)	12	39/4	49	8.11	10.31	2.20
12, b_2 ($n_-^\beta-b_2^+$)	2	54/36	44	8.46	10.64	2.18
16, a_1 (a_1^+)	15	6/4	79	8.60	10.92	2.32
7, a_2 (b_2^-)	0	4/2	96	8.68	11.13	2.45
11, b_2 ($b_2^++n_-^\beta$)	3	37/22	60	8.96	11.39	2.43
9, b_1 (b_1^-)	1	1/0	98	9.36	11.65	2.29
15, a_1 (b_1^+)	1	0	99	9.56	12.01	2.45
14, a_1 (n_+^β)	6	87/52	7	10.36	(12.7)	
6, a_2 (π_2^β)	1	88/50	11	10.40	(12.7)	
Compound III						
10, b_2 (π_5^X)	2	1/1	97/22	5.23	7.56	2.33
4, a_2 (π_4^X)	0	1/0	99/12	6.07	8.47	2.40
10, b_1 (π_3^β)	1	94/30	5/4	7.61	9.76	2.15
9, b_2 (π_3^X)	2	12/8	86/20	8.42	10.63	2.21
17, a_1 ($s^x-n_+^X$)	4	0	96/24	8.55	10.95	2.40
8, b_2 (n_-^β)	4	85/54	11/2	8.97	11.29	2.32
9, b_1 (n_-^X)	7	3/0	90/76	8.99	11.34	2.35
3, a_2 (π_2^X)	1	8/4	91/70	9.10	11.45	2.35
8, b_1 (σ^X)	0	1/0	99/14	9.51	11.81	2.30
16, a_1 ($\sigma^X+n_+^X$)	3	7/2	93/22	10.22	(12.5)	
15, a_1 (n_+^β)	8	83/50	7/2	10.61	(12.9)	
2, a_2 (π_2^β)	2	91/50	7/6	10.80	(13.1)	
7, b_2 (π_1^X)	2	20/5	78/31	11.12	(13.4)	

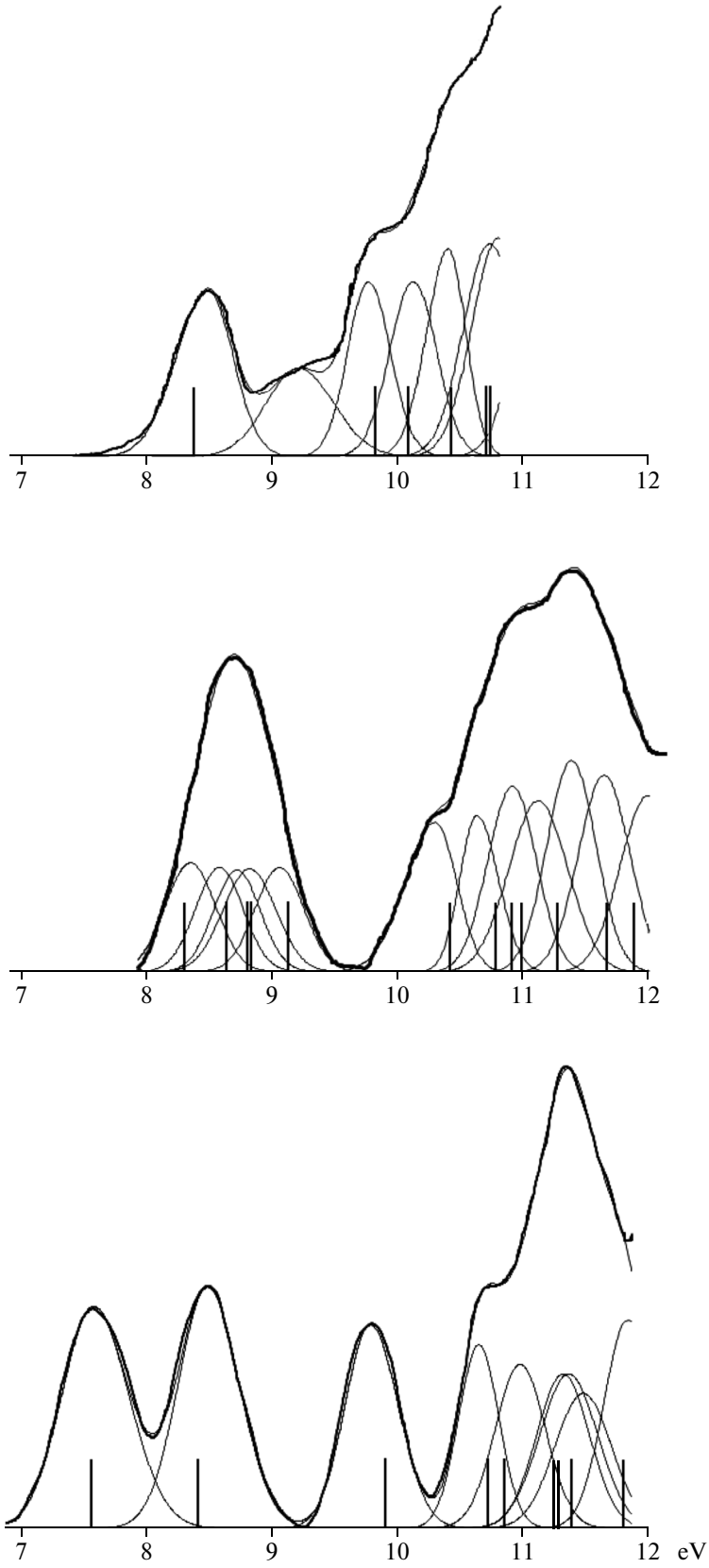

Fig. 1. Ultraviolet photoelectron spectra of compounds I–III.

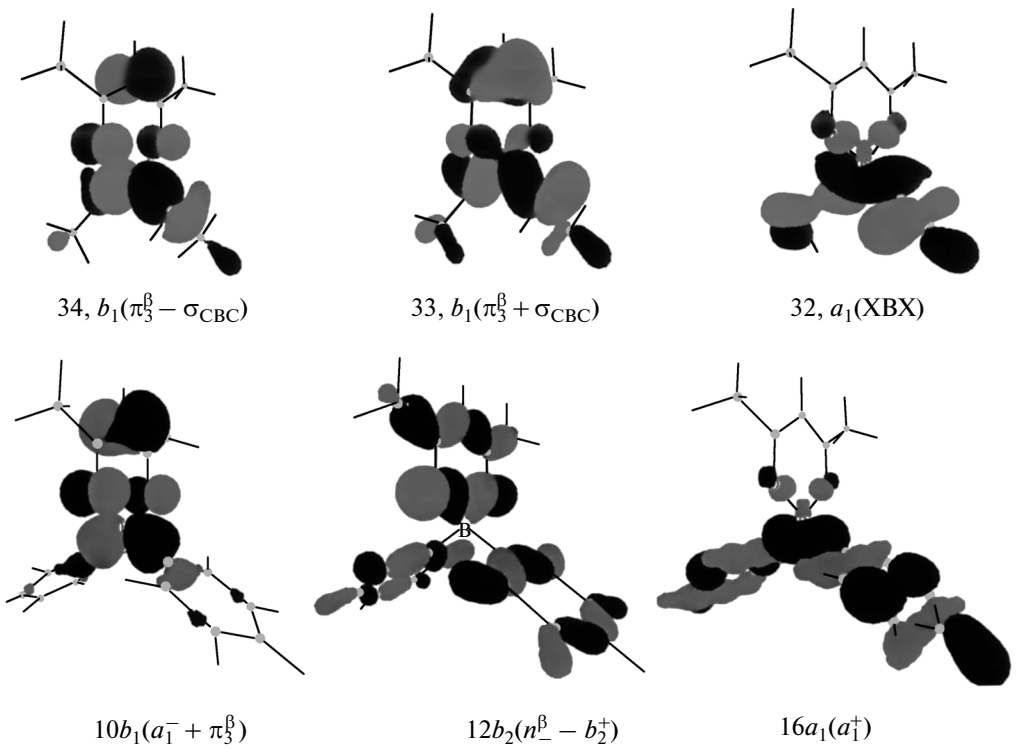

Fig. 2. Shape of the upper occupied molecular orbitals of compounds I (top) and II (bottom).

ment with the experimental data, showed the inclusion of a σ bonding orbital of C–B–C into the π system of the chelate ring, which coincides in symmetry with the π_3 orbital of the β-diketonate ligand (π_3^β). As shown in Fig. 2a and Table 2, the relative contributions of the π_3^β orbitals and the orbitals of the $B(C_2H_5)_2$ fragment to the bonding $b_1(\pi_3^\beta + \sigma_{CBC})$ and antibonding $b_1(\pi_3^\beta - \sigma_{CBC})$ MOs are similar, so that their net contribution to the covalent bond B–AA is nearly zero. The energy difference between the two higher occupied b_1 MOs, 1.44 eV, is in close agreement with the experimental value of $\Delta IE_{1-2} = 1.29$ eV (Table 2). The low-intensity "shoulder" within 9.0–9.5 eV, as assumed in [19], belongs to the products of the degradation of the sample formed during heating in a high vacuum. According to the calculations, the greatest contribution to the covalent bond C_2H_5–B–C_2H_5 comes from the fully symmetric MO $32a_1$ (XBX), 50% localized on the C–B–C atoms. The next, $b_2(n_-^\beta)$ MO is an antisymmetric combination of *n* orbitals of the oxygen atoms. According to calculations, on the energy scale between the $b_2(n_-^\beta)$ and $a_1(n_+^\beta)$ orbitals, there are four C–C- and C–H-bonding orbitals belonging to the two ethyl groups.

The values of IE_g obtained by expanding the spectral region from 8 to 11 eV for the six upper occupied MOs showed discrepancies with the values of $-\varepsilon_i$ not exceeding 0.1 eV, with an average deviation of δ_i from 2.19 eV of 0.05 eV (Table 2). Consequently, the ionization energies for deeper MOs can be estimated from ε_i values with an accuracy of 0.1 eV. In Table 2, these values are given in brackets for the MOs from 28 to 25, which are of interest in studying the effect of fragment X on the *n*- and π-levels of boron β-diketonate complexes.

According to quantum-chemical calculations, the first band in the ultraviolet photoelectron spectrum of compound II corresponds to five electronic levels, the upper four of which are localized on the phenyl groups. In the classification of the molecular orbitals of the two C_6H_5 groups (Table 2), we used both the C_{2v} symmetry of complex II and the local symmetry of C_6H_5 and $(C_6H_5)_2$ (Table 3). The superscripts "+" and "–" represent, respectively, the presence or absence of the nodal surface between the phenyl ring. The next two orbitals, $11b_1$ and $10b_1$, are similar in composition and nodal surface to the upper two b_1 orbitals of compound I (Fig. 2); herein, however, the π_3^β chelate orbital gives the dominant contribution to the $11b_1(\pi_3^\beta - a_1^-)$ antibonding MO (Table 2).

The second intense band in the photoelectron spectrum of II (Fig. 1) is caused by the photoionization of seven electronic levels. Among them, in addition to the bonding $10b_1(a_1^- + \pi_3^\beta)$ MO, are antibonding ($12b_2$) and bonding ($11b_2$) chelate combinations of

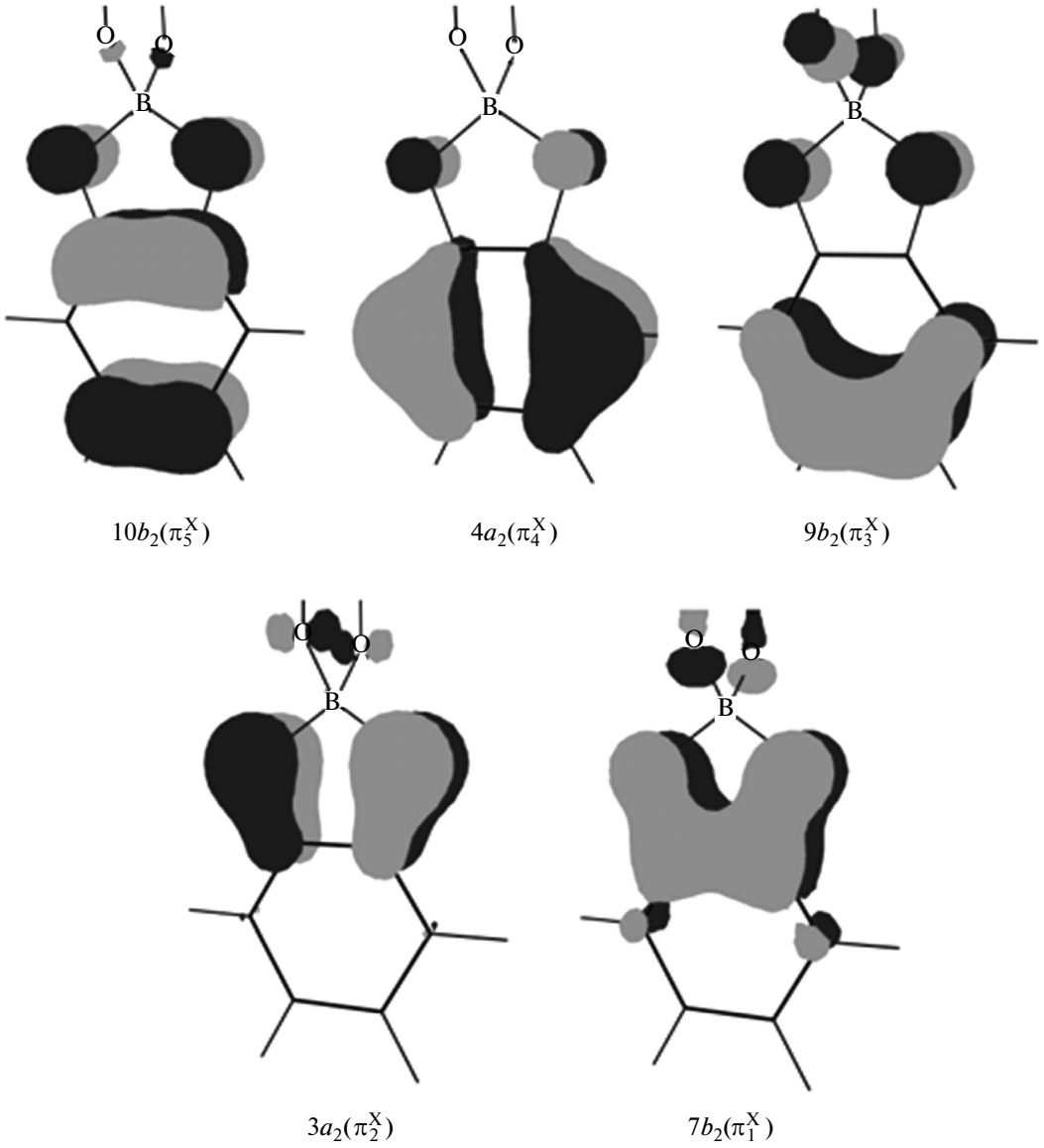

Fig. 3. Shape of the π molecular orbital of compound III.

the n_-^β chelate orbital with the b_2^+ orbital of the phenyl rings that correlates with the degenerate σ MO $2e_{2g}$ of benzene (Tables 2 and 3, Fig. 2). The four remaining MOs are localized mainly on the phenyl rings. The maximum contribution from the boron atom (15%) among the valence MOs in $16a_1(a_1^+)$ enables to associate it with the $32a_1$ bonding orbital of compound I. Using the above method, we estimated the ionization energies of the $14a_1(n_+^\beta)$ and $6a_2(\pi_2^\beta)$ chelate levels as 12.7 eV (Table 2).

In contrast to I and II, compound III has four oxygen atoms in the first coordination sphere of the boron. However, the calculation did not show a significant mixing of the electronic levels of the two chelating ligands (Table 2, Fig. 3). The first two bands in the photoelectron spectrum of compound III correspond to the two upper orbitals of the $C_6H_4O_2$ substituent, $10b_2(\pi_5^X)$ and $4a_2(\pi_4^X)$, representing antibonding combinations of the two upper π orbitals of the phenylene rings ($1e_{1g}$ in benzene) with the $2p$ orbitals of the oxygen. The lowering of the values of IE relative to C_6H_6 (9.24 eV) by 1.68 and 0.77 eV, respectively, occurs mainly due to the superposition of the negative effective charge (–0.94e in the NBO approximation, Table 4) onto the antibonding interaction of $2p\pi$ AOs of the oxygen and carbon (Fig. 3).

In accordance with the calculation results, closely consistent with the photoelectron spectrum, of the nine upper electron levels with IE < 12 eV, only two are

Table 3. Correlation of the symmetry of the MOs of benzene, phenyl groups (free and in compound II) (signs "+" and "–"indicate bonding and antibonding between phenyl groups)

C_6H_6, D_{6h}	C_6H_5, C_{2v}	$(C_6H_5)_2$	$(C_6H_5)_2BAA$, C_{2v}
$1e_{1g}(\pi)$	b_1	b_1^-	$b_1(b_1^-)$
		b_1^+	$a_1(b_1^+)$
	a_2	a_2^-	$a_2(a_2^-)$
		a_2^+	$b_2(a_2^+)$
$2e_{2g}(\sigma)$	a_1	a_1^-	–
		a_1^+	$a_1(a_1^+)$
	b_2	b_2^-	$a_2(b_2^-)$
		b_2^+	$b_2(b_2^+)$
$1a_{2u}(\pi)$	b_1	b_1^-	$b_1(b_1^-)$
		b_1^+	$a_1(b_1^+)$

located on the β-diketonate cycle. The values IE_3 = 9.76 eV for $10b_1(\pi_3^\beta)$ and IE_6 = 11.29 eV for $8b_2(n_-^\beta)$ (Table 2) coincide to within 0.1 eV with the corresponding values of IE in the photoelectron spectrum of F_2BAA (first two bands) [12]. The minor changes in the ionization energy of the π_3^β and n_-^β levels caused by the substitution of the $C_6H_4O_2$ aromatic group for the two acceptor fluorine atoms can be explained by similar values of the effective charges on β-diketonate ligand (Table 4).

According to the calculation results, the intense band with a maximum at 11.3 eV and a shoulder at 10.6 eV was expanded into six Gaussian MOs. In addition to the above-mentioned $8b_2(n_-^\beta)$ MO, these include two π orbitals, $9b_2(\pi_3^X)$ and $3a_2(\pi_2^X)$ (localized mainly on two $C_6H_4O_2$), and three σ-type MOs (Fig. 3, Table 2). The overlap population of the two B–O bonds of the substituent, exceeding by 35% the same parameter for the B–O bonds in the acetylacetonate cycle (Table 4), is mainly provided by the electrons belonging to the $17a_1$ and $9b_1$ MOs (Table 2). For the next four orbitals, from $16a_1$ to $7b_2$, the value of IE were estimated to within 0.1 eV of the values of ε_i and the mean value of $\delta_i = 2.32$ eV.

The effective charges and the orders of the B–O and B–X bonds listed in Table 4, show how substituents X influence the electron density distribution and covalent binding in the series of above X_2BAA acetylacetonates and F_2BAA boron difluoride. In the approximation of natural bond orbitals, the net negative charges on the X_2 are manyfold higher than charges on the AA. However, the high negative charge of the two oxygen atoms (–1.11...–1.14*e*), mainly due to the effect of the carbonyl carbon atom (Table 4), predetermines a high degree of ionicity of the bonds of the boron atom with the AA chelating ligand. The negative charges of the X substituents, from –0.62 to –0.94*e*, are in close agreement with the low values of IE for the π electrons of the benzene ring in compounds II and III as compared to benzene and its derivatives [9]. According to DFT calculations, the orders of the B–O bonds of the AA chelating ligand are 20–35% lower than the order of the B–C (compounds I, II) and B–O (compound III) bonds.

Thus, the DFT approximation used in the present paper (B3LYP5 functional in combination with the def2-TZVPP basis set) to study the electronic structure and to interpret the photoelectron spectra of acetylacetonates of three X_2B complexing agents showed a good correlation between the calculated and experimental energies of the MOs. For a set of 27 levels of the three compounds, the relationship between

Table 4. Total effective charges on the complexing agent and chelating ligand and bond orders in the first coordination sphere of the X_2BAA boron compounds

Compound	Effective charge, a.u.				Bond order	
	B	2X	AA/2O	$2C_\beta$	B–O	B–X
$(C_2H_5)_2BAA$	+0.86	–0.62	–0.24/–1.11	1.07	0.73	0.98
$(C_6H_5)_2BAA$	+0.82	–0.63	–0.19/–1.11	1.09	0.74	0.90
$(C_6H_4O_2)BAA$	+1.13	–0.94	–0.19/–1.12	1.07	0.80	1.08
F_2BAA	+1.21	–1.00	–0.21/–1.14	1.07	0.77	1.15

the ionization energy and the orbital energy $-\varepsilon$ is described by the equation: $IE = -1.00\varepsilon + 2.26$.

ACKNOWLEDGMENTS

This work was supported by the FEFU Scientific Foundation (grant no. 12-03-13008-16/13) and Federal Target Program "Research and Pedagogical Cadre for Innovative Russia (2009–2013)" (grant no. 14.A18.21.0792).

REFERENCES

1. A. G. Mirochnik, Doctoral Dissertation in Chemistry (Inst. Chemistry, Far Eastern Branch RAS, Vladivostok, 2007).
2. V. E. Karasev, A. G. Mirochnik, and E. V. Fedorenko, *Photophysics and Photochemistry of β-E-Diketonates of Boron Difluoride* (Dal'nauka, Vladivostok, 2006) [in Russian].
3. E. V. Fedorenko, I. B. L'vov, V. I. Vovna, et al., Russ. Chem. Bull. **60**, 1537 (2011).
4. G. Gorlitz, H. Hartmann, J. Kossanyi, et al., Ber. Bunsen-Ges. Phys. Chem. **102**, 1449 (1998).
5. S. J. Baker, T. Akama, Y. K. Zhang, et al., Bioorg. Med. Chem. Lett., No. 16, 5963 (2006).
6. A. Flores-Parra and R. Contreras, Coord. Chem. Rev. **196**, 85 (2000).
7. A. T. Balaban, C. Párkányi, I. Ghiviriga, et al., ARKIVOC **13**, 1 (2008).
8. V. I. Nefedov and V. I. Vovna, *The Electronic Structure of Chemical Compounds* (Nauka, Moscow, 1987) [in Russian].
9. V. I. Vovna, *Electronic Structure of Organic Compounds according to Photoelectron Spectroscopy Data* (Nauka, Moscow, 1991) [in Russian].
10. V. I. Vovna, Koord. Khim. **21**, 435 (1995).
11. A. V. Borisenko, V. I. Vovna, V. V. Gorchakov, et al., Zh. Strukt. Khim. **28**, 147 (1987).
12. V. I. Vovna, S. A. Tikhonov, and I. B. L'vov, Russ. J. Phys. Chem. A **85**, 1942 (2011).
13. V. I. Vovna, S. A. Tikhonov, and I. B. L'vov, Russ. J. Phys. Chem. A **87**, 688 (2013).
14. V. I. Vovna, M. V. Kazachek, and I. B. L'vov, Opt. Spectrosc. **112**, 497 (2012).
15. A. V. Borisenko and V. I. Vovna, *β-Diketonates of Metals* (Dal'nevost. Univ., Vladivostok, 1990), vol. 1, p. 178 [in Russian].
16. A. V. Borisenko, Candidate's Dissertation in Chemistry (Far Eastern State Univ., Vladivostok, 1990).
17. A. A. Granovsky, Firefly, Vers. 7.1.G. http://classic.chem.msu.su/gran/firefly/index.html.
18. K. Eichkorn, F. Weigend, O. Treutler, et al., Theor. Chem. Acc. **97**, 119 (1997).
19. Basis Set Exchange, Vers. 1.2.2. https://bse.pnl.gov/bse/portal
20. V. I. Vovna, V. V. Korochentsev, and A. A. Dotsenko, Koord. Khim. **37** (12), 38 (2011).
21. I. V. Krauklis and Yu. V. Chizhov, Opt. Spectrosc. **96**, 47 (2004).
22. I. V. Krauklis and Y. V. Chizhov, Opt. Spectrosc. **98**, 341 (2005).

Translated by V. Smirnov